

# A Component-Based Coding-Decoding Approach to Set-Membership Filtering for Time-Varying Systems Under Constrained Bit Rate <sup>★</sup>

Jun-Yi Li <sup>a</sup>, Zidong Wang <sup>b</sup>, Renquan Lu <sup>a,\*</sup>, Yong Xu <sup>a</sup>

<sup>a</sup> *Guangdong Province Key Laboratory of Intelligent Decision and Cooperative Control, School of Automation, Guangdong University of Technology, Guangzhou 510006, China*

<sup>b</sup> *Department of Computer Science, Brunel University London, Uxbridge, Middlesex, UB8 3PH, United Kingdom*

---

## Abstract

This paper is concerned with the set-membership filtering (SMF) problem for a class of discrete time-varying systems with unknown-but-bounded noises under bit rate constraints. The communication between sensor nodes and filters is implemented through a wireless digital communication network with limited bandwidth. A bit rate constraint is first established to quantify the extent to which the network is constrained. A component-based coding-decoding procedure is proposed that enables individual decoder to decode messages from different components scattering in different physical locations. Based on this procedure, a decoded-measurement-based recursive SMF scheme with a prediction-correction structure is put forward. The desired parameters of the set-membership filter can be calculated recursively by the proposed recursive SMF scheme. Furthermore, the co-design issue of the bit rate allocation protocol and the filter gain is converted into the mixed-integer nonlinear programming problem that is solved by means of the particle swarm optimization and the recursive filtering algorithms. Finally, numerical simulations on two scenarios are conducted to validate the effectiveness of the proposed SMF approach.

*Key words:* Constrained bit rate; component-based coding-decoding; set-membership filtering; co-design problem.

---

## 1 Introduction

The aim of the filtering problem is to extract the actual target state information from a series of observations that might be corrupted by various kinds of noises. For decades, the filtering problem has always been one of the most popular research topics in the communities of control and signal processing [2, 5, 10, 12, 13, 29, 38, 44, 45, 47, 50, 52]. In general, there are three categories of filtering schemes according to the types of the noises acting on the concerned systems [22, 32, 34, 36, 41, 46, 49, 56]. The first category is featured by the Kalman filter algorithm which is believed to be a reliable filtering method for systems subject to Gaussian noises. The second cat-

egory comprises the  $H_\infty$  filtering methods that are suitable for systems under energy-bounded noises and the main idea is to ensure given disturbance attenuation levels. The last category corresponds to the so-called set-membership filtering (SMF) scheme which is applicable to systems with unknown-but-bounded noises where a set of state estimates is provided to contain all possible actual states.

In the SMF schemes, estimation errors are guaranteed to fall into the obtained ellipsoidal set with 100% confidence. Since its first development in 1960s [3, 31, 42], the SMF has proven to be of great engineering importance for systems operating under unpredictable environmental changes, e.g. the networked control systems. As a result, a great number of researchers have devoted themselves to the study of the SMF problem for networked control systems and fruitful results have been reported in the literature [7, 15, 16, 18, 19, 21, 40, 55]. For instance, the set-membership state estimation problem has been investigated in [21] for a class of discrete time-varying nonlinear systems with uniform quantization effects under the maximum-error-first protocol. The SMF issues have been addressed in [7, 9, 16, 55] for time-varying systems under different transmission scheduling protocols in order to reduce the communication frequency.

Note that most existing results on the SMF problems of networked systems have been concerned with the ana-

---

<sup>★</sup> This work was supported in part by the National Natural Science Foundation of China (62121004, 62206063, 62141606 and 61933007), the Local Innovative and Research Teams Project of Guangdong Special Support Program of China (2019BT02X353), the Guangdong Basic and Applied Basic Research Foundation of China (2021A1515110765), the China Postdoctoral Science Foundation (2022M710825 and 2022T150146), the Royal Society of the UK, and the Alexander von Humboldt Foundation of Germany.

\* Corresponding author

*Email addresses:* [jun-yi-li@foxmail.com](mailto:jun-yi-li@foxmail.com) (Jun-Yi Li), [Zidong.Wang@brunel.ac.uk](mailto:Zidong.Wang@brunel.ac.uk) (Zidong Wang), [rqlu@gdut.edu.cn](mailto:rqlu@gdut.edu.cn) (Renquan Lu), [xuyong809@163.com](mailto:xuyong809@163.com) (Yong Xu).

log communication where the measurements are transmitted via the form of analog signals which take continuous values with infinite precision. With the rapid development of modern control equipments and network technologies, the analog communication has been quickly replaced by the digital communication which is capable of meeting the needs for reliable, secure and real-time communication. In wireless digital communication, sensors are often subject to sampling, quantization, and coding before transmission [6, 27, 28, 54]. Although sampling and quantization of sensor signals have already received considerable attention in networked control systems, the coding-decoding procedure (CDP) has not received much attention and this is particularly true for the SMF issues.

The CDP is designed to implement the conversion between numeric data and codewords consisting of 0 and 1, where the coding intends to map numeric data to specific codewords, while the decoding aims at restoring the codewords to the original numerical data as accurately as possible according to certain rules. In recent years, the coding-decoding communication scheme has drawn much research attention due to its irreplaceable role in the digital communication [14, 17, 20, 23, 39, 51, 53]. It should be pointed out that in most relevant literature on coding-decoding communication, a common assumption is that parameters of the CDP maintain the same for all system states/outputs of interest. Unfortunately, such an assumption is not always reasonable as different components of the state/output vector may have different requirements for data resolution in practice. For instance, the alphabet of a larger size is more suitable for components requiring high-accuracy data.

Although the component-based CDP (CBCDP) is more practical for networked systems, its wide application in practice still confronts several challenges. In the existing CDPs, a decoder only needs to decode the information from the corresponding coder. Comparatively, in the case of the CBCDP, the decoder is required to receive and decode messages from different sensors. Consequently, it is required that the CBCDP should endow the decoder with the ability to decode the codewords from different coders. However, up to now, the SMF issue under CBCDP has not been properly examined yet. Therefore, it is the primary motivation of this paper to study the SMF problem with the CBCDP.

In digital communication networks, the bit rate is defined as the number of bits transmitted over a digital communication network per second, and is a critical measure for characterizing the network bandwidth. For a typical network system with multiple nodes, although the total bit rate of the network is large, each node is usually allocated with only a small portion of the total bit rate, and this leads to the inevitable bit rate constraints. Consequently, the side-effect of limited bit rate has become a critical issue and has attracted much research interest in the field of networked systems. Initial research on this issue has focused on finding out how the constrained bit rate affects the system dynamics [26]. For

example, the connections between the minimum bit rate (that ensures system stability) and the unstable eigenvalue (of the open-loop system), known as the data rate theorem, have been uncovered in [24, 25, 37, 43] for various systems. However, little attention has been paid to quantitatively model the degree of network constraint, not to mention the case where the impact from the network constraints on the SMF performance is quantitatively analyzed. This constitutes the second motivation of our present investigation.

Based on the above discussions, it can be concluded that the SMF problem for networked systems with constrained bit rate remains open due to the following three main challenges: 1) how to construct a mathematical model accounting for not only the bandwidth limits of the entire network but also the bandwidth allocation for each node? 2) how to develop a CBCDP to fit the need of real networks? and 3) how to design the filter parameters according to certain SMF performance requirements? These identified challenges motivate us to find satisfactory answers.

In this paper, we endeavor to deal with the SMF problem for discrete time-varying systems with constrained bit rate. The primary contributions are summarized from the following four aspects.

- (1) For the SMF problem with limited communication bandwidth, a bit rate constraint model is, for the first time, introduced to characterize the bandwidth allocation of the network.
- (2) A component-based coding-decoding scheme is developed to enable each node to decode information from different nodes.
- (3) The SMF problem is investigated for the discrete time-varying systems with a component-based coding-decoding strategy and the desired parameters of the set-membership filter are obtained by solving a mixed-integer nonlinear programming (MINP) problem with the bit rate as a co-design parameter.

**Notation:** In this paper,  $\mathbb{R}^n$  and  $\mathbb{R}^{n \times m}$  stand for  $n$  dimensional Euclidean space and the set of  $n \times m$  real matrices, respectively.  $\mathbb{N}$ ,  $\mathbb{N}^+$ , and  $\mathbb{R}$  denote the sets of non-negative integers, positive integers, and real numbers, respectively.  $\text{diag}_N\{A_i\}$  and  $\text{col}_N(e_i)$  denote diagonal block matrix  $\text{diag}_N\{A_1, A_2, \dots, A_N\}$  and column vector  $[e_1^T, e_2^T, \dots, e_N^T]^T$ , separately.  $M \oplus N$  represents the elementwise sum of the sets  $M$  and  $N$ . The notation  $X > Y$  ( $X \geq Y$ ) denotes that  $X - Y$  is positive definite (semi-positive definite), where  $X$  and  $Y$  are symmetric matrices. For any  $z \in \mathbb{R}^n$ ,  $z^T$  and  $\|z\|_2$  are its transpose and its Euclidean norm.

## 2 Problem Formulation and Preliminaries

### 2.1 System description

Consider the following discrete time-varying system:

$$x_{k+1} = A_k x_k + B_k w_k \quad (1)$$

where  $x_k \in \mathbb{R}^{n_x}$  is the state vector of the plant,  $w_k \in \mathbb{R}^{n_w}$  refers to the process disturbance signal,  $A_k \in \mathbb{R}^{n_x \times n_x}$  and  $B_k \in \mathbb{R}^{n_x \times n_w}$  are time-varying matrices. Before proceeding further, we introduce the following assumption.

**Assumption 1** *The initial state  $x_0$  satisfies the following condition:*

$$x_0 \in \mathcal{E}(\hat{x}_{0|0}, P_{0|0}) \triangleq \{x_0 \in \mathbb{R}^{n_x} : (x - \hat{x}_{0|0})^T P_{0|0}^{-1} (x - \hat{x}_{0|0}) \leq 1\} \quad (2)$$

where  $\hat{x}_{0|0}$  is the estimation of the initial state and  $\mathcal{E}(b, Q)$  represents an ellipsoidal set with the center  $b$  and the shape matrix  $Q > 0$ .

Without loss of generality, we assume that the sensors measuring the system states are divided into  $n_y$  sensor nodes according to their spatial distribution. In this case, the measurements are described as

$$\begin{cases} y_{1,k} = C_{1,k} x_k + D_{1,k} v_k \\ y_{2,k} = C_{2,k} x_k + D_{2,k} v_k \\ \vdots \\ y_{n_y,k} = C_{n_y,k} x_k + D_{n_y,k} v_k \end{cases} \quad (3)$$

where  $y_{i,k} \in \mathbb{R}$  ( $i \in \mathbb{N}_{n_y}^+ \triangleq \{1, 2, \dots, n_y\}$ ) means the one-dimensional measurement output of sensor  $i$ ,  $v_k \in \mathbb{R}^{n_v}$  refers to the measurement noises,  $C_{i,k} \in \mathbb{R}^{1 \times n_x}$  and  $D_{i,k} \in \mathbb{R}^{1 \times n_v}$  are time-varying matrices.

**Assumption 2** *The process noise  $w_k$  and the measurement noise  $v_k$  are unknown but confined to the following ellipsoidal sets:*

$$\begin{cases} \mathcal{W}_k \in \mathcal{E}(0, W_k) \triangleq \{w_k \in \mathbb{R}^{n_w} : w_k^T W_k^{-1} w_k \leq 1\} \\ \mathcal{V}_k \in \mathcal{E}(0, V_k) \triangleq \{v_k \in \mathbb{R}^{n_v} : v_k^T V_k^{-1} v_k \leq 1\} \end{cases} \quad (4)$$

where  $W_k$  and  $V_k$  are known positive definite matrices with appropriate dimensions.

### 2.2 The description of bit rate

In this paper, the information is transmitted via the noise-free wireless digital communication network under constrained bit rate. The bit rate of the whole network is usually limited due to resource constraints on the underlying hardware and network environment. Accordingly,

only a fraction of the total bit rate is allocated to each node according to certain allocation rules. The model of bit rate constraint can be expressed as follows:

$$R_s \geq \sum_{i=1}^{n_y} R_i \quad (5)$$

where  $R_s \in \mathbb{N}^+$  represents the total available bit rate determined by the network device and  $R_i \in \mathbb{N}$  denotes the allocated bit rate of sensor node  $i$ .

**Remark 1** *In a typical networked system, the media access control (MAC) protocol accounts for the allocation of communication bandwidths and plays a critical role in the operation of the entire network. The design principle of MAC is to allocate the communication resources among network nodes in a fair and efficient manner. Based on the way that network resources are allocated among nodes, MAC protocols can be categorized into two types: the competition-based MAC and allocation-based MAC protocols [33, 48]. It has been evidenced that, compared with the competition-based MAC protocols, the allocation-based MAC protocols (which allocate each node's available bandwidth according to a specific rule) are more effective in reducing packet collision in large-scale networks [1, 30]. Therefore, in this paper, we consider the case that the available bit rate for each node is allocated by a allocation protocol satisfying (5).*

### 2.3 CBCDP under constrained bit rate

To comply with the digital communication fashion, a coding-decoding strategy subject to constrained bit rate condition (5) is presented in this subsection. By using a coder, the measurement of each accessible node is coded as a string of binary codes selected from the alphabet  $\mathbb{A}^{R_i}$  of size  $2^{R_i}$ .

In practice, different components of the state/output vector may have different data resolution requirements. As such, a CBCDP is designed in this paper.

#### 1) Coding procedure of sensor node $i$ .

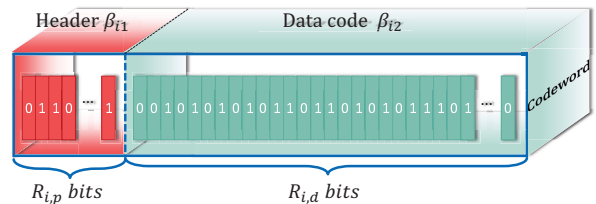


Fig. 1. The bits allocation of sensor node  $i$

In the coding procedure, the node label  $i$  (the simplified IP address) and the measurement data  $y_{i,k}$  are introduced into the codeword, respectively. As such, each sensor node's available bits are divided into two parts

defined by header  $\beta_{i1}$  and data code  $\beta_{i2}$  at each coding instant  $k$ . The number of bits allocated to code the header part  $\beta_{i1}$  is defined as:

$$R_{i,p} = \lceil \log_2 n_y \rceil \quad (6)$$

where  $n_y$  is the number of sensor nodes measuring the system state, and  $\lceil \log_2 n_y \rceil$  is the minimum integer greater than or equal to  $\log_2 n_y$ , which denotes the minimum number of bits required to represent the integer  $n_y$  by binary coding. An integer  $s_0^i$  is determined by binary encoding with  $\lceil \log_2 n_y \rceil$  bits, which is also the first element of the codeword  $\mathcal{Y}_{i,k}^{R_i}$  to be defined later. Noting that once  $n_y$  is determined, the number of bits used to describe the first part of each node stays the same, which suggests that

$$R_{1,p} = R_{2,p} = \dots = R_{n_y,p} \triangleq R_p = \lceil \log_2 n_y \rceil. \quad (7)$$

**Remark 2** *In contrast to the existing coding methods [23, 39, 53], we spent  $R_p$  bits to code the labels of the nodes. With this procedure, although the resolution of the transmitted data degrades, the effectiveness of the decoding procedure is guaranteed with the specific requirement that the decoder is able to decode messages from different nodes.*

In view of (6) and (7), the number of available bits for the data code part  $\beta_{i2}$  is given as

$$R_{i,d} = R_i - R_p = R_i - \lceil \log_2 n_y \rceil \quad (8)$$

which determines the maximum number of quantization levels.

The following uniform quantizer is introduced in this paper to facilitate the CBCDP. For the quantizer of sensor node  $i$ , given a scaling parameter  $b_i > 0$ , the quantization region is identified subsequently by  $\mathcal{B}_{b_i} = \{y_i \in \mathbb{R} : |y_i| \leq b_i\}$ . By choosing an integer  $q_i$  as the quantization level, the  $\mathcal{B}_{b_i}$  will be partitioned into  $q_i$  intervals  $I_{s_1^i}^i(b_i)$ , with  $s_1^i \in \{1, 2, \dots, q_i\}$  and

$$\begin{aligned} I_1^i(b_i) &\triangleq \left\{ y_i \mid -b_i \leq y_i < -b_i + \frac{2b_i}{q_i} \right\} \\ I_2^i(b_i) &\triangleq \left\{ y_i \mid -b_i + \frac{2b_i}{q_i} \leq y_i < -b_i + \frac{4b_i}{q_i} \right\} \\ &\vdots \\ I_{q_i}^i(b_i) &\triangleq \left\{ y_i \mid b_i - \frac{2b_i}{q_i} \leq y_i \leq b_i \right\}. \end{aligned} \quad (9)$$

---

### Algorithm 1 Coding procedure of sensor $i$

---

- ▶ **Step 1.** Given measurement  $y_{i,k}$ , allocated bit rate  $R_i$ , the number of sensors  $n_y$ , and the scaling parameter  $b_i$ .
  - ▶ **Step 2.** Calculate the value of  $R_{i,p}$  from equation (7).
  - ▶ **Step 3.** Calculate the value of  $R_{i,d}$  from equation (8).
  - ▶ **Step 4.** Obtain the first component  $s_0^i$  of the codeword by using the node label.
  - ▶ **Step 5.** Calculate the largest number of quantization levels  $q_{im}$  based on equation (10).
  - ▶ **Step 6.** Obtain an integer  $s_1^i$  such that  $y_{i,k} \in I_{s_1^i}^i(b_i)$ .
  - ▶ **Step 7.** Obtain and output the codeword  $\mathcal{Y}_{i,k}^{R_i}$  with the form of  $[s_0^i, s_1^i]$ .
- 

For the uniform quantizers described above, in order to ensure that the information corresponding to each interval is uniquely coded, the maximum number of quantization levels is defined as:

$$q_{im} = 2^{R_{i,d}} = 2^{R_i - R_p}. \quad (10)$$

Then, for each  $\mathcal{B}_{b_i}$ , the center of the interval  $I_{s_1^i}^i(b_i)$  is denoted by

$$\bar{h}_{b_i}^i(s_1^i) \triangleq -b_i + [((2s_1^i - 1) b_i) / 2^{R_{i,d}}]. \quad (11)$$

Hence, for any  $y_i \in \mathcal{B}_{b_i}$ , there exists a certain integer  $s_1^i \in \{1, 2, \dots, q_i\}$  such that  $y_i \in I_{s_1^i}^i$ , which satisfies the following inequality:

$$|y_i - \bar{h}_{b_i}^i(s_1^i)| \leq \frac{b_i}{2^{R_{i,d}}}. \quad (12)$$

The integer  $s_1^i$  is the remaining fraction of the codeword in the coding procedure.

In summary, for  $y_{i,k} \in I_{s_1^i}^i(b_i) \subset \mathcal{B}_{b_i}$ , the following codeword is generated

$$\mathcal{Y}_{i,k}^{R_i} = [s_0^i, s_1^i] \quad (13)$$

where  $s_0^i$  refers to the sensor node label and  $s_1^i$  represents the data measured by sensor node  $i$ . The detailed coding procedure is presented in Algorithm 1.

### 2) Decoding procedure.

For any codeword  $\mathcal{Y}_{x,k}^{R_x} = [s_0^x, s_1^x]$  received from a sensor node, the node label  $l_s$  is firstly extracted by the follow-

ing procedure:

$$l_s \triangleq \begin{bmatrix} s_0^x & s_1^x \\ 0 \end{bmatrix}. \quad (14)$$

When the first component of  $\mathcal{Y}_{l_s, k}^{R_{l_s}}$  is identified, the data part can be decoded by using the corresponding alphabet  $\mathbb{A}^{R_{l_s}}$  embedded in the decoder. In addition, the output of the decoder is defined as

$$\check{y}_{i,k} = h_{b_{l_s}}^{l_s}(s_1^{l_s}) = -b_{l_s} + \left[ \left( (2s_1^{l_s} - 1) b_{l_s} \right) / 2^{R_{l_s}} \right]. \quad (15)$$

The decoding procedure is shown in detail in Algorithm 2.

---

**Algorithm 2** Decoding procedure

---

- ▶ **Step 1.** If there is a codeword  $\mathcal{Y}_{j,k}^{R_j}$ ,  $j = 1, 2, \dots, n_y$ , then go to the next step, else go to Step 6.
  - ▶ **Step 2.** Extract the node label  $l_s$  via equation (14).
  - ▶ **Step 3.** Obtain the parameters  $b_{l_s}$  and  $q_{l_{sm}}$  by looking up the corresponding code alphabet.
  - ▶ **Step 4.** Obtain the decoded measurement  $\check{y}_{j,k}$  by (15).
  - ▶ **Step 5.** If there is another codeword  $\mathcal{Y}_{j,k}^{R_j}$ ,  $j = 1, 2, \dots, n_y$ , then go to Step 2, else go to Step 6.
  - ▶ **Step 6.** Stop.
- 

#### 2.4 Decoded-measurement-based SMF

Denoting  $C_k \triangleq \text{col}_{n_y}(C_{i,k})$ ,  $D_k \triangleq \text{col}_{n_y}(D_{i,k})$  and  $y_k \triangleq \text{col}_{n_y}(y_{i,k})$ , the measurement (3) of time-varying system (1) is rearranged as:

$$y_k = C_k x_k + D_k v_k. \quad (16)$$

Based on the CBCDP proposed in subsection 2.3, the remote filter is capable of receiving measurements with the following form at time instant  $k$  from  $n_y$  sensor nodes:

$$\check{y}_k = \begin{bmatrix} -b_1 + [((2s_1^1 - 1) b_1) / 2^{R_{1,a}}] \\ -b_2 + [((2s_1^2 - 1) b_2) / 2^{R_{2,a}}] \\ \vdots \\ -b_{n_y} + [((2s_1^{n_y} - 1) b_{n_y}) / 2^{R_{n_y,a}}] \end{bmatrix}. \quad (17)$$

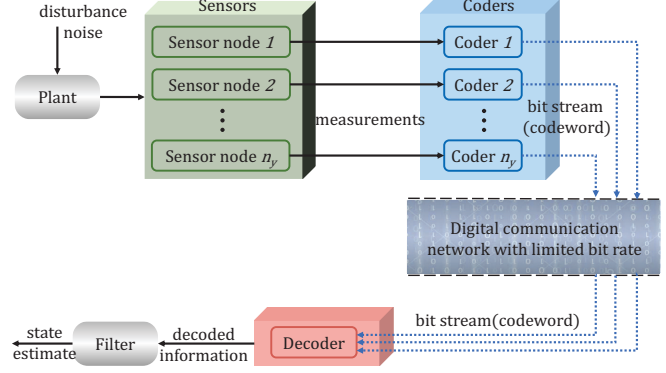


Fig. 2. Schematic of filtering problem subject to CBCDP

Let  $d_{i,k} \triangleq \check{y}_{i,k} - y_{i,k}$  be the decoding error of sensor node  $i$  and  $d_k \triangleq \check{y}_k - y_k = \text{col}_{n_y}(d_{i,k})$ . It follows from (12) and (17) that

$$d_{i,k}^T d_{i,k} \leq \frac{b_i^2}{(2^{R_i - \lceil \log_2 n_y \rceil})^2} \triangleq \bar{d}_{i,k} \quad (18)$$

$$d_k^T d_k \leq \sum_{i=1}^{n_y} \frac{b_i^2}{(2^{R_i - \lceil \log_2 n_y \rceil})^2} \quad (19)$$

and  $d_k \in \mathcal{E}(0, \bar{d}_k)$  with  $\bar{d}_k = \text{diag}\{\bar{d}_{1,k}, \bar{d}_{2,k}, \dots, \bar{d}_{n_y,k}\}$ .

In this paper, the set-membership filtering for time-varying system (1) with constrained bit rate condition (5) is investigated by using decoded measurements. The schematic structure is shown in Fig. 2.

The two main objectives of this article are stated as follows.

- (1) For the time-varying system (1), let the set of bit rate  $R_i \in \mathbb{N}^+$  ( $i = 1, 2, \dots, n_y$ ) be given. Our first objective is to design a recursive SMF scheme with prediction-correction structure that employs the decoded measurement such that the target state  $x_k$  lies in

$$\mathcal{E}(\hat{x}_{k|k}^*, P_{k|k}^*) = \{x_k \in \mathbb{R}^{n_x} : (x_k - \hat{x}_{k|k}^*)^T (P_{k|k}^*)^{-1} (x_k - \hat{x}_{k|k}^*) \leq 1\} \quad (20)$$

with  $\hat{x}_{k|k}^*$  and  $P_{k|k}^*$  are two parameters to be designed.

- (2) An optimization problem is to be investigated to minimize  $P_{k|k}$  in the sense of matrix trace at each time instant where the available bit rate of each node is designable.

### 3 Main Results

Based on the established CBCDP under the constrained bit rate, in this section, a decoded-measurement-based

set-membership filter is first designed to estimate the ellipsoid of the system state. Subsequently, the filter parameters and the bit rate allocation protocol are recursively obtained by solving an optimization problem. Before proceeding further, the following lemma is recalled to facilitate the derivation of our main results.

**Lemma 1** *For an ellipsoid  $z \in \mathcal{E}(b, Q)$ , the affine transformation  $z \mapsto Bz + c$  with known matrices  $B$  and vectors  $c$  is also an ellipsoid and satisfies*

$$Bz + c \in B\mathcal{E}(b, Q) + c = \mathcal{E}(Bb + c, BQB^T).$$

**Lemma 2** *The elementwise sum of given ellipsoids  $\mathcal{E}(b_i, Q_i)$  ( $i = 1, 2, \dots, m$ ) can be enveloped by a bounded ellipsoid*

$$\mathcal{E}(b_1, Q_1) \oplus \mathcal{E}(b_2, Q_2) \oplus \dots \oplus \mathcal{E}(b_m, Q_m) \subseteq \mathcal{E}(b, Q).$$

with the center  $b = \sum_{i=1}^m b_i$  and the shape matrix

$$Q = \left( \sum_{i=1}^m \alpha_i \right) \left( \sum_{i=1}^m \alpha_i^{-1} Q_i \right) \quad \forall \alpha_i > 0.$$

### 3.1 Design of decoded-measurement-based SMF

In the following theorem, a decoded-measurement-based recursive SMF which features a prediction-correction structure, is proposed to estimate the ellipsoid of the system state.

**Theorem 1** *Consider the bit rate condition (5) and the CBCDP described in Algorithms 1 and 2. Suppose that the system state  $x_k$  lies in the ellipsoid  $\mathcal{E}(\hat{x}_{k|k}^*, P_{k|k}^*)$  and the positive integers  $R_s, R_i$  ( $i \in \mathbb{N}_{n_y}^+$ ) be given. The system state  $x_{k+1}$  obtained by (1) with decoded measurements  $\check{y}_k$  is enclosed in the ellipsoid  $\mathcal{E}(\hat{x}_{k+1|k+1}, P_{k+1|k+1})$  with the following parameters:*

$$\begin{aligned} \hat{x}_{k+1|k+1} &= \hat{x}_{k+1|k} + K_{k+1} \bar{e}_{k+1} \\ P_{k+1|k+1} &= \Pi_{k+1} (I - K_{k+1} C_{k+1}) P_{k+1|k} \end{aligned} \quad (21)$$

where

$$\begin{aligned} \bar{e}_{k+1} &= \check{y}_{k+1} - C_{k+1} \hat{x}_{k+1|k}, \quad \hat{x}_{k+1|k} = A_k \hat{x}_{k|k}^* \\ P_{k+1|k} &= (1 - \lambda_k)^{-1} A_k P_{k|k} A_k^T + \lambda_k^{-1} B_k W_k B_k^T \\ \Xi_{k+1} &= \mu_{k+1}^{-1} \check{D}_{k+1} + C_{k+1} P_{k+1|k} C_{k+1}^T \\ \Pi_{k+1} &= 1 + \mu_{k+1} - \bar{e}_{k+1}^T \Xi_{k+1}^{-1} \bar{e}_{k+1} \\ K_{k+1} &= P_{k+1|k} C_{k+1}^T \Xi_{k+1}^{-1} \end{aligned} \quad (22)$$

with any  $\mu_{k+1} > 0$  and  $\lambda_k \in (0, 1)$ .

**Proof:** First, it follows from Lemma 1, Lemma 2 and system dynamics (1) that

$$x_{k+1} = A_k x_k + B_k w_k$$

$$\begin{aligned} &\in \mathcal{E}(A_k \hat{x}_{k|k}, A_k P_{k|k} A_k^T) \oplus \mathcal{E}(0, B_k W_k B_k^T) \\ &\subseteq \mathcal{E}(\hat{x}_{k+1|k}, \Phi(P_{k|k}, W_k, \lambda_k)) \end{aligned} \quad (23)$$

with

$$\Phi(P_{k|k}, W_k, \lambda_k) = (1 - \lambda_k)^{-1} A_k P_{k|k} A_k^T + \lambda_k^{-1} B_k W_k B_k^T.$$

Therefore, it can be concluded that

$$x_{k+1} \in \mathcal{E}(\hat{x}_{k+1|k}, P_{k+1|k}). \quad (24)$$

Next, the decoded measurement  $\check{y}_{k+1}$  is applied to establish the parameters for the ellipsoid in (24). One can obtain from (3) and (17) that

$$\begin{aligned} &\check{y}_{k+1} - C_{k+1} x_{k+1} \\ &= y_{k+1} + d_{k+1} - C_{k+1} x_{k+1} \\ &= D_{k+1} v_{k+1} + d_{k+1} = \check{D}_{k+1} \bar{D}_{k+1} \in \mathcal{E}(0, \hat{D}_{k+1}) \end{aligned} \quad (25)$$

with  $\check{D}_{k+1} = [I_{n_y}, D_{k+1}]$ ,  $\bar{D}_{k+1} = [d_{k+1}^T, v_{k+1}^T]^T$ , and  $\hat{D}_{k+1} = \text{diag}\{\bar{d}_{k+1}, V_{k+1}\}$ . Then, all possible values of  $x_{k+1}$  that are compatible with the decoded measurements could be constrained to the set

$$\mathcal{X}_{k+1} = \left\{ x_{k+1} \mid C_{k+1} x_{k+1} \in \mathcal{E}(\check{y}_{k+1}, \check{D}_{k+1}) \right\} \quad (26)$$

with  $\check{D}_{k+1} = \check{D}_{k+1} \hat{D}_{k+1} \check{D}_{k+1}^T$ . It is obvious that  $x_{k+1} \in \mathcal{E}(\hat{x}_{k+1|k}, P_{k+1|k}) \cap \mathcal{X}_{k+1}$ . Thus, the design of the set-membership filter for the system state  $x_{k+1}$  turns into the determination of  $\hat{x}_{k+1|k+1}$  and  $P_{k+1|k+1}$  in the following set

$$\begin{aligned} &\mathcal{U}_{set}(x_{k+1}) \\ &\triangleq \left\{ x_{k+1} \mid x_{k+1} \in \mathcal{E}(\hat{x}_{k+1|k}, P_{k+1|k}), x_{k+1} \in \mathcal{X}_{k+1} \right\} \\ &\subseteq \mathcal{E}(\hat{x}_{k+1|k+1}, P_{k+1|k+1}) \end{aligned} \quad (27)$$

where  $\mathcal{E}(\hat{x}_{k+1|k+1}, P_{k+1|k+1})$  is the outer approximation of  $\mathcal{E}(\hat{x}_{k+1|k}, P_{k+1|k}) \cap \mathcal{X}_{k+1}$ . To solve the parameters mentioned above, we build the following auxiliary set

$$\begin{aligned} &\mathcal{A}_{set}(x_{k+1}) \\ &\triangleq \left\{ x_{k+1} \mid (x_{k+1} - \hat{x}_{k+1|k})^T P_{k+1|k}^{-1} (x_{k+1} - \hat{x}_{k+1|k}) \right. \\ &\quad \left. + \mu_{k+1} (C_{k+1} x_{k+1} - \check{y}_{k+1})^T \check{D}_{k+1}^{-1} \right. \\ &\quad \left. \times (C_{k+1} x_{k+1} - \check{y}_{k+1}) \leq 1 + \mu_{k+1} \right\} \end{aligned} \quad (28)$$

for any  $\mu_{k+1} \geq 0$ . It follows from the results of [31] that  $\mathcal{U}_{set}(x_{k+1}) \subseteq \mathcal{A}_{set}(x_{k+1})$ . Furthermore,  $\mathcal{A}_{set}(x_{k+1})$  satisfies the following form:

$$\mathcal{A}_{set}(x_{k+1}) \subseteq \mathcal{E}(\hat{m}_{k+1}, \hat{S}_{k+1}) \quad (29)$$

where  $\hat{m}_{k+1}$  represents the midpoint with the form:

$$\hat{m}_{k+1} = \hat{x}_{k+1|k} + \mu_{k+1} \mathcal{R}_{k+1}^{-1} C_{k+1}^T \check{D}_{k+1}^{-1} \bar{e}_{k+1} \quad (30)$$

and  $\hat{S}_{k+1}$  refers to the shape matrix with the form:

$$\hat{S}_{k+1} = \gamma_{k+1}^2 \mathcal{R}_{k+1}^{-1} \quad (31)$$

with

$$\begin{aligned} \mathcal{R}_{k+1} &= P_{k+1|k}^{-1} + \mu_{k+1} C_{k+1}^T \check{D}_{k+1}^{-1} C_{k+1} \\ \gamma_{k+1}^2 &= -\mu_{k+1} \check{y}_{k+1}^T \check{D}_{k+1}^{-1} \check{y}_{k+1} \\ &\quad - \hat{x}_{k+1|k}^T P_{k+1|k}^{-1} \hat{x}_{k+1|k} \\ &\quad + \varpi_{k+1}^T \mathcal{R}_{k+1}^{-1} \varpi_{k+1} + 1 + \mu_{k+1} \\ \varpi_{k+1} &= P_{k+1|k}^{-1} \hat{x}_{k+1|k} + \mu_{k+1} C_{k+1}^T \check{D}_{k+1}^{-1} \check{y}_{k+1}. \end{aligned} \quad (32)$$

Applying the matrix inverse lemma, it is readily seen that

$$\begin{aligned} \mathcal{R}_{k+1}^{-1} &= P_{k+1|k} - P_{k+1|k} C_{k+1}^T \Xi_{k+1}^{-1} C_{k+1} P_{k+1|k} \\ &= (I - P_{k+1|k} C_{k+1}^T \Xi_{k+1}^{-1} C_{k+1}) P_{k+1|k} \\ &= (I - K_{k+1} C_{k+1}) P_{k+1|k} \end{aligned} \quad (33)$$

$$\Xi_{k+1}^{-1} = \mu_{k+1} \check{D}_{k+1}^{-1} - \mu_{k+1}^2 \check{D}_{k+1}^{-1} C_{k+1} \mathcal{R}_{k+1}^{-1} C_{k+1}^T \check{D}_{k+1}^{-1}. \quad (34)$$

In view of the above discussions, one has

$$\begin{aligned} K_{k+1}^{-1} &= P_{k+1|k} C_{k+1} \Xi_{k+1}^{-1} \\ &= \mu_{k+1} P_{k+1|k} C_{k+1} \check{D}_{k+1}^{-1} \\ &\quad - \mu_{k+1}^2 P_{k+1|k} C_{k+1} \check{D}_{k+1}^{-1} C_{k+1} \mathcal{R}_{k+1}^{-1} C_{k+1}^T \check{D}_{k+1}^{-1} \\ &= \mu_{k+1} P_{k+1|k} (\mathcal{R}_{k+1} - \mu_{k+1} C_{k+1}^T \check{D}_{k+1}^{-1} C_{k+1}) \\ &\quad \times \mathcal{R}_{k+1}^{-1} C_{k+1}^T \check{D}_{k+1}^{-1} \\ &= \mu_{k+1} \mathcal{R}_{k+1}^{-1} C_{k+1}^T \check{D}_{k+1}^{-1} \end{aligned} \quad (35)$$

which means that the midpoint satisfies

$$\hat{m}_{k+1} = \hat{x}_{k+1|k} + K_{k+1}^{-1} \bar{e}_{k+1} \triangleq \hat{x}_{k+1|k+1}. \quad (36)$$

Moreover, the parameter  $\gamma_{k+1}$  can be rewritten in a similar way to the result of [31] as

$$\gamma_{k+1} = \sqrt{1 + \mu_{k+1} - \bar{e}_{k+1}^T \Xi_{k+1}^{-1} \bar{e}_{k+1}}. \quad (37)$$

By integrating what are described in (28)-(37), we can obtain the required ellipsoid (21), and the proof is thus complete.

**Remark 3** In Theorem 1, a decoded-measurement-based recursive SMF with prediction step (24) and correction step (26) is provided to estimate the system state subject to the CBCDP. It should be noted that all the key elements leading to the complexity in filter design have been covered in Theorem 1 which include 1) time-varying parameters of the system; 2) the allocated bit rate of each sensor node; and 3) the parameters related to the component-based coding-decoding strategy. In the following sections, we will further explore the co-design issue of the bit rate allocation protocol and the filter parameter to improve the SMF performance.

### 3.2 Co-design of decoded-measurement-based set-membership filter and bit rate allocation protocol

It can be found from Theorem 1 that the set of the allocated bit rate  $R_i$  ( $i \in \mathbb{N}_{n_y}^+$ ) plays a vital role in (21). On the other hand, the available bit rates are designable parameters assigned by the MAC protocol in response to the required performance. Therefore, the co-design issue of the bit rate allocation protocol and filter parameters will be the emphasis of the remainder of this paper. The following minimization problem subject to variable  $R_i$  ( $i \in \mathbb{N}_{n_y}^+$ ) is proposed to deal with the co-design issue.

**OP :** The optimization problem is to minimize the ellipsoid constraint  $P_k$  (in the sense of the matrix trace) for the most accurate filtering performance under bit rate constraint condition (5) with known total available bit rate  $R_s$  and variable allocated bit rate  $R_i$ . Such a problem is addressed in Theorem 2.

**Theorem 2** Consider bit rate condition (5), system (1), and the CBCDP described in Algorithms 1 and 2. Suppose that the system state  $x_k$  lies in the ellipsoid  $\mathcal{E}(\hat{x}_{k|k}^*, P_{k|k}^*)$  and the positive integers  $R_s$  be given. The system state  $x_{k+1}$  obtained by (1) is enclosed in the ellipsoid  $\mathcal{E}(\hat{x}_{k+1|k+1}, P_{k+1|k+1})$  with the parameters described in (21), where positive integers  $R_i$  ( $i \in \mathbb{N}_{n_y}^+$ ) are the solution to the following OP:

$$\begin{aligned} \min_{P_{k+1}, K_{k+1}, \bar{R}_{k+1}} & \text{Trace}\{P_{k+1}\} \\ \text{s.t.} & (5), (21) \\ & 0 \leq R_{i,k+1} \leq R_s \\ & R_{i,k+1} \in \mathbb{N}, i = 1, 2, \dots, n_y \end{aligned} \quad (38)$$

where  $\bar{R}_{k+1} = \{R_{1,k+1}, R_{2,k+1}, \dots, R_{n_y,k+1}\}$ .

Note that the presented co-design problem in Theorem 2 is an MINP problem which is difficult to be solved due to the integer constraints of  $R_i$  and the nonlinear term in equality constraints (21).

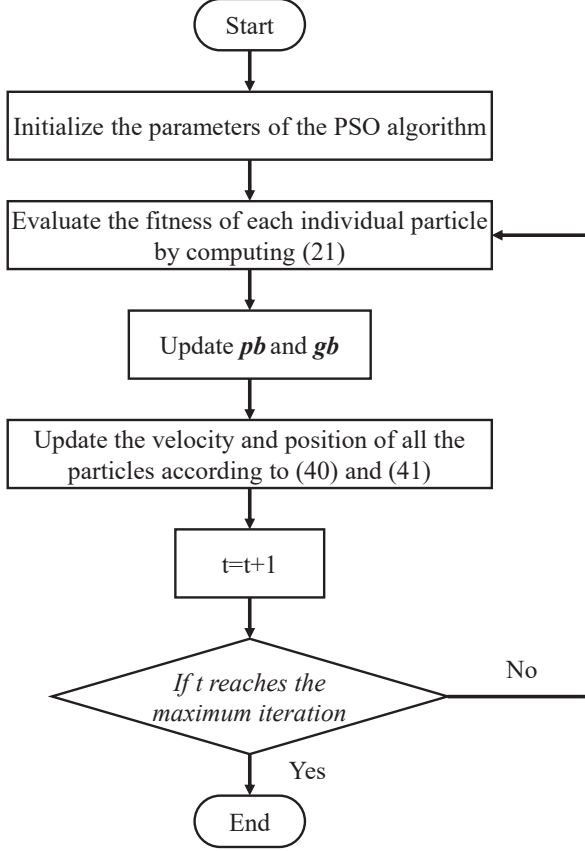


Fig. 3. Flowchart of the PSO-Assisted co-design algorithm

To cope with such an MINP problem, an algorithm that combines the PSO and Kalman-like recursive filtering algorithm is presented in the following stage. For the optimization problem (38) with constraints, we first introduce a penalty function that transforms (38) into the following form:

$$\begin{aligned}
 \min_{P_{k+1}, K_{k+1}, \bar{R}_{k+1}} \quad & \text{Trace}\{P_{k+1}\} + f_p(R) \\
 \text{s.t.} \quad & (21) \\
 & R_{i,k+1} \in \mathbb{N}, \quad i = 1, 2, \dots, n_y
 \end{aligned} \quad (39)$$

where  $f_p(R) = \max\{0, \sum_{i=1}^{n_y} R_{i,k+1} - R_s\}$  is the penalty function with  $R = [R_{1,k+1}, R_{2,k+1}, \dots, R_{n_y,k+1}]$ . The fitness function of PSO is defined as  $\text{Trace}\{P_{k+1}\} + f_p(R)$ .

Denote  $\mathbf{v}_i = [\mathbf{v}_{i,1}, \mathbf{v}_{i,2}, \dots, \mathbf{v}_{i,n_y}]$  and  $\mathbf{R}_i = [\mathbf{R}_{i,1}, \mathbf{R}_{i,2}, \dots, \mathbf{R}_{i,n_y}]$  as the velocity and the position of the particle  $i$ , respectively. The velocity and the position updating equations of particle  $i$  are given as follows:

$$\mathbf{v}_i(t+1) = \mathbf{w}\mathbf{v}_i(t) + \mathbf{c}_1\mathbf{r}_1(\mathbf{p}_i(t) - \mathbf{R}_i(t)) + \mathbf{c}_2\mathbf{r}_2(g_b(t) - \mathbf{R}_i(t)) \quad (40)$$

$$\mathbf{R}_i(t+1) = \mathbf{R}_i(t) + \mathbf{v}_i(t+1) \quad (41)$$

where  $t$  is the iteration number,  $\mathbf{p}_i$  represents the historical individual best position ( $p_b$ ) for particle  $i$ , and  $g_b$  bespeaks the historical global best position for the entire swarm,  $\mathbf{c}_1$  and  $\mathbf{c}_2$  refer to the cognitive acceleration coefficient and the social acceleration coefficient, separately,  $\mathbf{w}$  denotes the inertia weight. Keeping in mind that the PSO algorithm in this paper is designed to solve the MINP problem with integer variables  $R_i$ , the initial position and velocity of the particle, as well as the parameters  $\mathbf{c}_1$ ,  $\mathbf{c}_2$  and  $\mathbf{w}$  are all selected as integers in the algorithm. Moreover,  $\mathbf{r}_1$  and  $\mathbf{r}_2$  are two integers that are chosen randomly from 1 or 2.

From the flowchart depicted in Fig. 3, it can be seen that the first step is to initialize the parameters of the PSO algorithm, including  $\mathbf{N}_S$ ,  $\mathbf{N}_I$ ,  $\mathbf{c}_1$ ,  $\mathbf{c}_2$ ,  $\mathbf{w}$ , along with the velocity  $\mathbf{V}_i$ , the position  $\mathbf{R}_i$  and the initial  $\mathbf{p}_i$  of each particle. The second step is to evaluate each particle's fitness function  $\mathbf{F}(\mathbf{R}_i)$  by computing the equations (21). If the equations (21) is infeasible, the value of the fitness will be artificially assigned a sufficiently large value ( $10^4$  in this paper) to mitigate the influence of the relevant particles on the particle swarm. The third step is to update the  $g_b$  by choosing the smaller one between  $\mathbf{F}(\mathbf{R}_i)$  and  $\mathbf{F}(\mathbf{p}_i)$  and to update the  $p_b$  by choosing the minimum fitness value in the swarm. The fourth step is to update the velocity and the position of each particle by the given updating equations (40) and (41). Each iteration repeats the process from the second step to the fourth step until the maximum number of iterations is reached. Then, select the  $g_b$  as the parameters of bit rate allocation protocol. At last, based on the selected bit rate protocol, parameters of the set-membership filter are produced by computing the equations (21).

**Remark 4** As a matter of fact, the bit rate allocation protocol is a problem-dependent parameter that can be designed according to different application requirements. On the other hand, it can be readily observed from Theorem 1 that the parameters  $R_i$  ( $i \in \mathbb{N}_{n_y}^+$ ) play a significant role in the design of the set-membership filter. Therefore, Theorem 2 investigates the co-design problem of the bit rate allocation protocol and the filter parameters. Such a co-design problem is further transformed into an MINP problem that can be well solved by combining the PSO algorithm and the Kalman-like recursive filtering algorithm. The complexity of PSO-Assisted co-design algorithm is  $\mathbf{N}_S\mathbf{N}_I\mathcal{O}((1+n_x+n_w+n_v+n_y))$ , which is determined by the PSO algorithm and the Kalman-like recursive filtering algorithm. Fortunately, with the increase in computer computing power and the accelerated development of PSO technology, the problems of the computational burden and the local extremes of the algorithm in online mode are promising to be well solved.

**Remark 5** In this paper, the SMF problem is investigated for discrete time-varying systems with constrained bit rate. The bandwidth limitation of the communication network is characterized by introducing a bit rate constraint model (5). A CBCDP is proposed to meet the requirements of the decoder for decoding messages from dif-



ferent components, and a design method is later proposed in Theorem 1 to compute the decoded-measurement-based set-membership filter. In order to further reduce the filtering error, a co-design procedure of the bit rate protocol and filter parameters is presented in Theorem 2.

**Remark 6** This paper represents the first attempt to investigate the SMF problems for time-varying systems with unknown-but-bounded noises and CBCDP within a digital communication network framework. Compared to the existing literature, the main novelties of our current results lie in 1) the established bit rate condition, which relies on the bandwidth allocation protocol, is new in the sense of characterizing the bandwidth limit of the communication network for the addressed SMF problem; 2) the proposed component-based coding-decoding strategy is new, which makes it possible for the filter to decode information from each sensor; and 3) the design algorithms for the set-membership filter parameters are new through solving an MINP problem with the bit rate as a co-design parameter.

**Remark 7** From the methodological viewpoint, we would like to clarify that a) the proposed coding method is new in that  $R_p$  bits are utilized to code the labels of the nodes in the component-based coding-decoding scheme; b) the proposed decoding method is new in that specific requirements on the decoding procedure can be guaranteed so that the decoder is able to decode messages from different nodes; and c) the co-design method is new for the interdisciplinary problem crossing communication and filtering areas.

## 4 Numerical Example

In this section, two numerical examples are provided to demonstrate the validity of the proposed set-membership filtering scheme for systems (1) subject to CBCDP and bit rate constraints.

The time-varying system (1) is considered in this section with the following parameters:

$$A_k = 0.1 \begin{bmatrix} A_{11,k} & -0.1 & A_{13,k} \\ 0.42 & A_{22,k} & 0.25 \\ -0.2 & A_{32,k} & 0.8 \end{bmatrix}, B_k = \begin{bmatrix} 0.6 \\ 0.6 \\ 0.9 \end{bmatrix}$$

$$A_{11,k} = 0.85 + \sin(0.5k)$$

$$A_{13,k} = -0.1 + 4 \sin(0.5k)$$

$$A_{22,k} = 0.7 + \sin(0.4k)$$

$$A_{32,k} = -0.2 + 2 \cos(0.4k).$$

The sensors of this system is categorized into 2 sensor

nodes and its measurement model is given below.

$$\begin{cases} y_{1,k} = \begin{bmatrix} 0.3 + 0.2 \sin(0.3k) & 0.21 & 0.3 \end{bmatrix} x_k \\ \quad + (0.3 + 0.1 \sin(0.3k)) v_k \\ y_{2,k} = \begin{bmatrix} -0.09 & 0.3 & 0.3 + 0.1 \cos(0.4k) \end{bmatrix} x_k \\ \quad + (0.4 + 0.2 \sin(0.4k)) v_k. \end{cases}$$

The noises are selected to be  $w_k = 0.6 \sin(0.3k)$  and  $v_k = 0.1 \sin(0.2k)$ . Then,  $W$  and  $V$  can be chosen as 0.36 and 0.01, respectively. It can then be readily verified that  $w_k$  and  $v_k$  belong to the set of ellipsoids defined in (4). Let the initial state of system and filter be  $x_0 = [2, -2, -2]$ ,  $\hat{x}_0 = [0, 0, 0]$ . The initial constraint is set to be  $P_0 = \text{diag}\{16, 16, 16\}$ . Then, it can also be verified that the provided initial conditions satisfy Assumption 1. The parameter  $\lambda$  is set as [9],  $\mu$  is set to be  $\mu = 30$ .

For the coding procedure outlined in Algorithm 1, the scaling parameters are selected to be  $b_1 = 0.8$  and  $b_2 = 0.5$ . In the following, two cases are given to prove the validity of the set-membership filter design method proposed in this paper.

### Case 1: Filtering effects of Theorem 1 and Theorem 2.

This case illustrates the effects of Theorem 1 and Theorem 2 on designing the set-membership filter, including the effects on the upper bound and the effects on the filtering error. The total bit rate is assumed to be  $R_s = 16$  bps. The available bit rate of each sensor node is allocated as  $R_1 = 3$  and  $R_2 = 13$  in Theorem 1. In Theorem 2, the available bit rate is determined by solving (39) and the detailed parameters are shown in Table 1.

Table 1  
The bit rate allocation of node 1 and node 2

k	1	...	7	...	13	...	19	...	21	...	30
$R_1$	9	...	8	...	9	...	8	...	6	...	8
$R_2$	7	...	8	...	7	...	8	...	7	...	8

The simulation results are depicted in Figs. 4-9, where Figs. 4-6 depict the trajectories of system states and their estimates under Theorem 1 and Theorem 2; Figs. 7-9 plot their upper bounds and lower bounds under Theorem 1 and Theorem 2. From Figs. 4-6, we observe that the state trajectories of the filter obtained by solving the Theorem 2 are more close to the trajectories of the true state in most of the time. It can be readily observed from Figs. 7-9 that by applying Theorem 2, one can obtain smaller bounds in most of the time compared to Theorem 1. The simulation results confirm the following two aspects: 1) the SMF performance can be satisfied by solving Theorem 1 and Theorem 2; and 2) a better filtering performance can be obtained through the proposed co-design problem (Theorem 2).

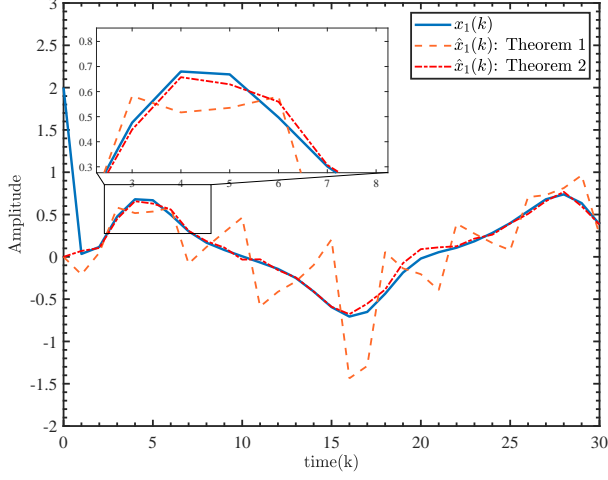


Fig. 4. The trajectories of  $x_{1,k}$  and  $\hat{x}_{1,k}$  subject to Theorem

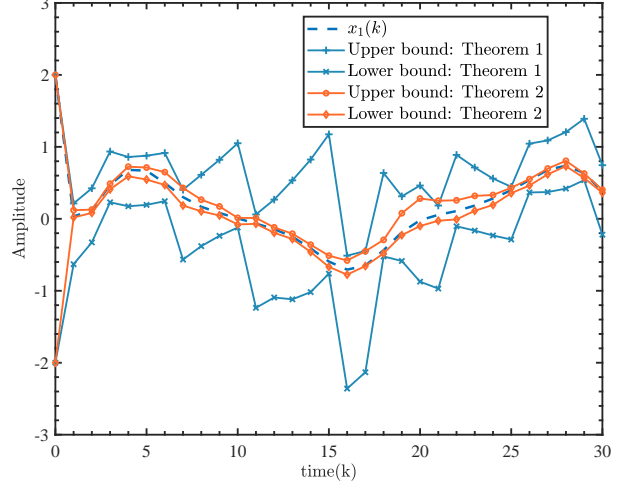


Fig. 7. The upper and lower bounds of state  $\hat{x}_{1,k}$  subject to

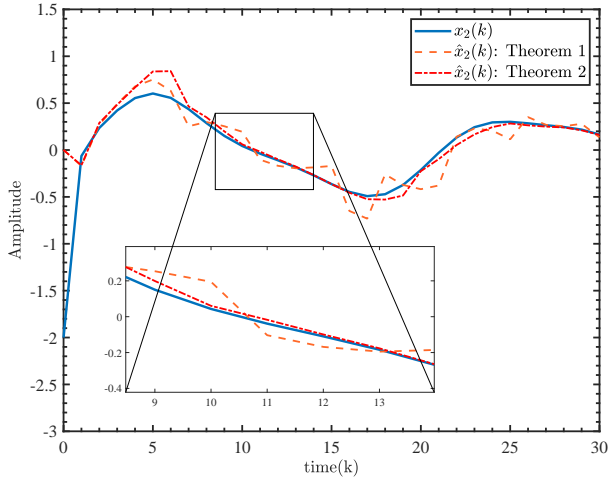


Fig. 5. The trajectories of  $x_{2,k}$  and  $\hat{x}_{2,k}$  subject to Theorem

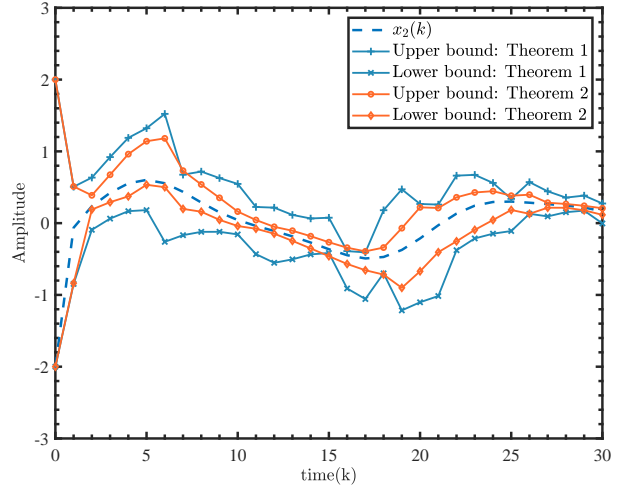


Fig. 8. The upper and lower bounds of state  $\hat{x}_{2,k}$  subject to Theorem 1 and Theorem 2

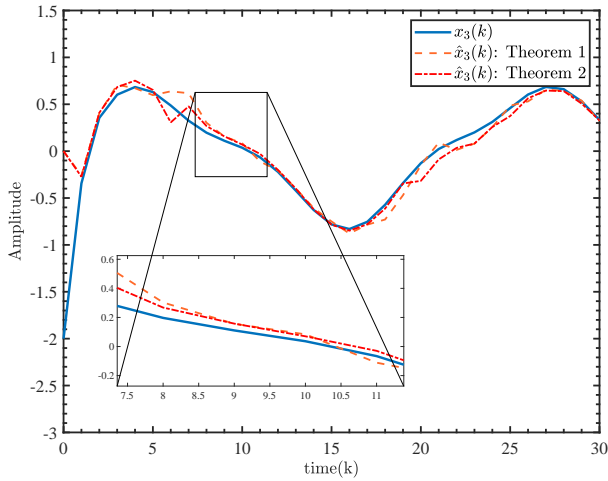


Fig. 6. The trajectories of  $x_{3,k}$  and  $\hat{x}_{3,k}$  subject to Theorem 1 and Theorem 2

Case 2: Effect of total available bit rate  $R_s$  on filtering performance.

This case is intended to clarify the effect of the total available bit rate on the design of the set-membership filter. First, four simulations are carried out with total bit rates of  $R_s = 8$  bps,  $R_s = 16$  bps,  $R_s = 32$  bps, and  $R_s = 64$  bps, respectively. The average filtering error  $\bar{e}_k$  under different available bit rate  $R_s$  are shown in Fig. 10, where  $\bar{e}_k = \|e_k\|_2 / n$ , and  $n$  is the simulation run length ( $n = 30$  in this paper). Two observations can be obtained from Fig. 10: 1) as the available bit rate increases, the filtering error becomes smaller; 2) when the bit rate increases to a certain level, its effect on the filtering error becomes smaller.

Next, two simulations are conducted with  $R_s = 8$  bps and  $R_s = 16$  bps, respectively. The available bit rate of each sensor node is allocated by an average allocation protocol, i.e.,  $R_1 = R_2 = \frac{R_s}{2} = 4$  bps in case  $R_s = 8$

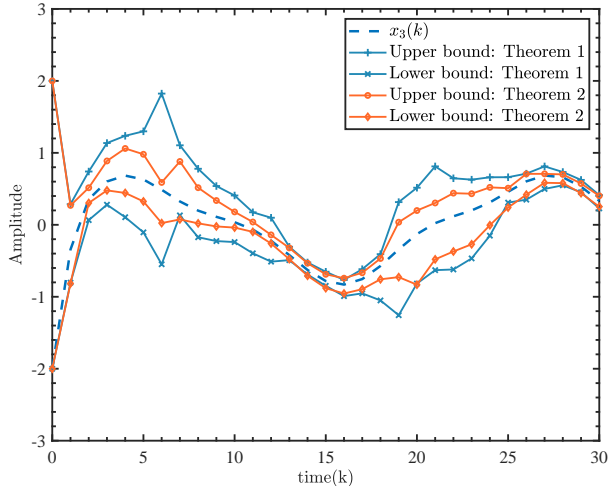


Fig. 9. The upper and lower bounds of state  $\hat{x}_{3,k}$  subject to Theorem 1 and Theorem 2

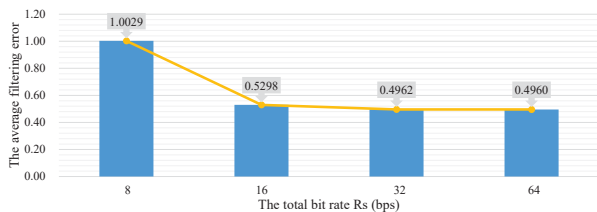


Fig. 10. The average filtering errors  $\bar{e}_k$  with  $R_s = 8$  bps,  $R_s = 16$  bps,  $R_s = 32$  bps, and  $R_s = 64$  bps

bps and  $R_1 = R_2 = \frac{R_s}{2} = 8$  bps in case  $R_s = 16$  bps. The corresponding simulation results are shown in Figs. 11-13, which depict the filtering errors and their upper bounds under different available bit rate. It can be readily seen from Figs. 11-13 that one can obtain lower upper bounds and lower filtering errors in most of the time under the condition  $R_s = 16$  bps. This is reasonable because a higher bit rate allows us to provide more quantization levels in the design of the coding procedure, which will result in lower decoding errors. As a result, the measurements can be restored more completely at the receiver for filter design, thereby improving the filtering performance.

## 5 Conclusions

In this paper, we have investigated the SMF problem for a discrete time-varying system with constrained bit rate. A bit rate constraint has been introduced to characterize the limits of the network bandwidth and the allocation of each node. A CBCDP procedure has been proposed to guarantee the uniqueness of the coding-decoding procedure. After establishing the CBCDP under the constrained bit rate condition, a decoded-measurements-based recursive filter has been developed to estimate the plant subject to the unknown-but-bounded noises. The design issue of the filter has been addressed by solving an OP, which is a MINP problem with the bit rate as a co-design parameter. The effectiveness of the proposed

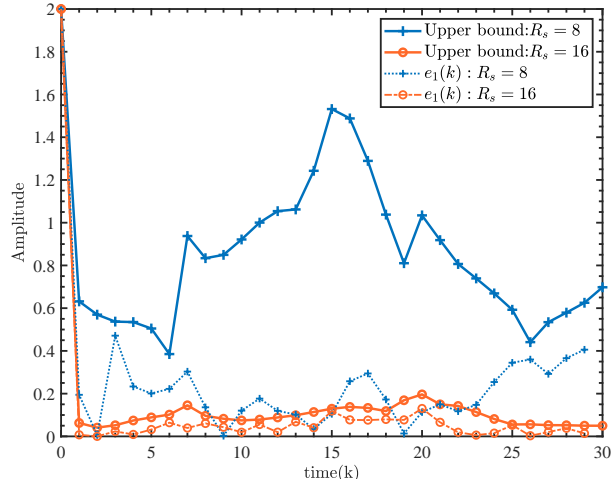


Fig. 11. The filtering errors  $\|e_{1,k}\|_2$  and the upper bounds subject to different bit rate

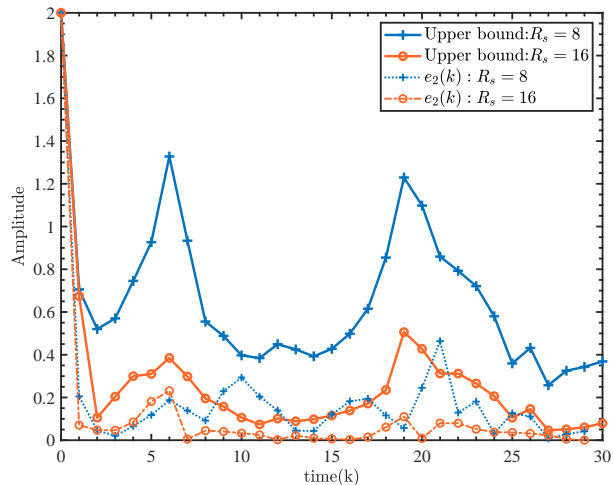


Fig. 12. The filtering errors  $\|e_{2,k}\|_2$  and the upper bounds subject to different bit rate

filter design scheme has been illustrated through two numerical cases. Finally, we may extend the results of this paper to other kinds of filtering problems (e.g. moving horizon estimation [8, 35]), and this gives us future research topics.

## References

- [1] A. S. Althobaiti and M. Abdullah, Medium access control protocols for wireless sensor networks classifications and cross-layering, *Procedia Computer Science*, vol. 65, pp. 4–16, 2015.
- [2] N. W. Bauer, M. C. F. Donkers, N. Van De Wouw, and W. P. M. H. Heemels, Decentralized observer-based control via networked communication, *Automatica*, vol. 49, no. 7, pp. 2074–2086, 2013.
- [3] D. P. Bertsekas and I. B. Rhodes, Recursive state estimation for a set-membership description of uncertainty, *IEEE Transactions on Automatic control*, vol. 16, no. 2, pp. 117–128, 1971.

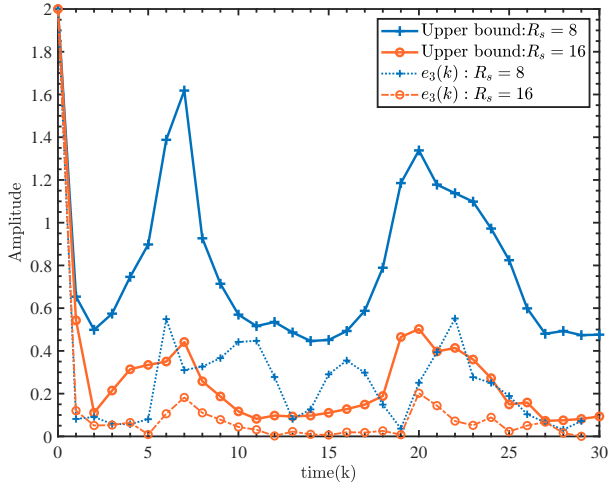


Fig. 13. The filtering errors  $\|e_{3,k}\|_2$  and the upper bounds subject to different bit rate

[4] S. Boyd, L. El Ghaoui, E. Feron, and V. Balakrishnan, *Linear Matrix Inequalities in System and Control Theory*. SIAM, 1994.

[5] R. Caballero-Aguila, A. Hermoso-Carazo, and J. Linares-Perez, Optimal state estimation for networked systems with random parameter matrices, correlated noises and delayed measurements, *International Journal of General Systems*, vol. 44, no. 2, pp. 142–154, 2015.

[6] J. Cao, D. Ding, J. Liu, E. Tian, S. Hu and X. Xie, Hybrid-triggered-based security controller design for networked control system under multiple cyber attacks, *Information Sciences*, vol. 548, pp. 69–84, 2021.

[7] F. Yao, Y. Ding, S. Hong and S.-H. Yang, A survey on evolved LoRa-based communication technologies for emerging internet of things applications, *International Journal of Network Dynamics and Intelligence*, vol. 1, no. 1, pp. 4-19, Dec. 2022.

[8] Y. Chen, J. Ren, X. Zhao and A. Xue, State estimation of Markov jump neural networks with random delays by redundant channels, *Neurocomputing*, vol. 453, pp. 493–501, 2021.

[9] D. Ding, Z. Wang, and Q.-L. Han, A set-membership approach to event-triggered filtering for general nonlinear systems over sensor networks, *IEEE Transactions on Automatic Control*, vol. 65, no. 4, pp. 1792–1799, 2020.

[10] M. Fu, C. E. De Souza, and Z. Q. T. Luo, Finite-horizon robust Kalman filter design, *IEEE Transactions on Signal Processing*, vol. 49, no. 9, pp. 2103–2112, 2001.

[11] L. El Ghaoui and G. Calafiore, Robust filtering for discrete-time systems with bounded noise and parametric uncertainty, *IEEE Transactions on Automatic control*, vol. 46, no. 7, pp. 1084–1089, 2001.

[12] X. Wang, Y. Sun and D. Ding, Adaptive dynamic programming for networked control systems under communication constraints: a survey of trends and techniques, *International Journal of Network Dynamics and Intelligence*, vol. 1, no. 1, pp. 85-98, Dec. 2022.

[13] J. Lam, B. Zhang, Y. Chen, and S. Xu, Robust stabilization of MIMO systems in finite/fixed time, *International Journal of Robust and Nonlinear Control*, vol. 25, pp. 269–281, 2015.

[14] W. Li, Y. Niu and Z. Cao, Event-triggered sliding mode control for multi-agent systems subject to channel fading, *International Journal of Systems Science*, vol. 53, no. 6, pp. 1233-1244, 2022.

[15] X. Li, G. Wei, and L. Wang, Distributed set-membership filtering for discrete-time systems subject to denial-of-service attacks and fading measurements: A zonotopic approach, *Information Science*, vol. 547, pp. 49–67, 2021.

[16] J. Li, G. Wei, D. Ding, and Y. Li, Set-membership filtering for discrete time-varying nonlinear systems with censored measurements under Round-Robin protocol, *Neurocomputing*, vol. 281, pp. 20–26, 2018.

[17] T. Li and L. Xie, Distributed coordination of multi-agent systems with quantized-observer based encoding-decoding, *IEEE Transactions on Automatic Control*, vol. 57, no. 12, pp. 3023–3037, 2012.

[18] L. Liu, L. Ma, J. Zhang and Y. Bo, Distributed non-fragile set-membership filtering for nonlinear systems under fading channels and bias injection attacks, *International Journal of Systems Science*, vol. 52, no. 6, pp. 1192–1205, 2021.

[19] L. Liu, L. Ma, J. Guo, J. Zhang and Y. Bo, Distributed set-membership filtering for time-varying systems: A coding-decoding-based approach, *Automatica*, vol. 129, art. no. 109684, 2021.

[20] W. Liu, Z. Wang and M. Ni, Controlled synchronization for chaotic systems via limited information with data packet dropout, *Automatica*, vol. 49, no. 8, pp. 2576–2579, 2013.

[21] S. Liu, G. Wei, Y. Song, and D. Ding, Set-membership state estimation subject to uniform quantization effects and communication constraints, *Journal of Franklin Institute*, vol. 354, no. 15, pp. 7012–7027, 2017.

[22] P. Lu, B. Song and L. Xu, Human face recognition based on convolutional neural network and augmented dataset, *Systems Science & Control Engineering*, vol. 9, no. s2, pp. 29-37, 2021.

[23] J. Mao, Y. Sun, X. Yi, H. Liu and D. Ding, Recursive filtering of networked nonlinear systems: A survey, *International Journal of Systems Science*, vol. 52, no. 6, pp. 1110–1128, Jan. 2021.

[24] G. N. Nair and R. J. Evans, Exponential stabilisability of finite-dimensional linear systems with limited data rates, *Automatica*, vol. 39, no. 4, pp. 585–593, 2003.

[25] G. N. Nair and R. J. Evans, Stabilizability of stochastic linear systems with finite feedback data rates, *SIAM Journal on Control and Optimization*, vol. 43, no. 2, pp. 413–436, 2004.

[26] G. N. Nair, F. Fagnani, S. Zampieri and R. J. Evans, Feedback control under data rate constraints: An Overview, *Proceedings of the IEEE*, vol. 95, no. 1, pp. 108–137, 2007.

[27] C. Peng, D. Yue and M. R. Fei, A higher energy-efficient sampling scheme for networked control systems over IEEE 802.15.4 wireless networks, *IEEE Transactions on Industrial Informatics*, vol. 12, no. 5, pp. 1766–1774, 2015.

[28] C. Peng, Q.-L. Han and D. Yue, Communication-delay-distribution-dependent decentralized control for large-scale systems with IP-based communication networks, *IEEE Transactions on Control Systems Technology*, vol. 21, no. 3, pp. 820–830, 2012.

[29] F. Qu, X. Zhao, X. Wang and E. Tian, Probabilistic-constrained distributed fusion filtering for a class of time-varying systems over sensor networks: A torus-event-triggering mechanism, *International Journal of Systems Science*, vol. 53, no. 6, pp. 1288-1297, 2022.

[30] I. Rhee, A. Warriar, M. Aia, J. Min and M. L. Sichitiu, Z-MAC: A hybrid MAC for wireless sensor networks, *IEEE/ACM Transactions on Networking*, vol. 16, no. 3, pp. 511–524, 2008.

[31] F. C. Scheppe, Recursive state estimation: Unknown but bounded errors and system inputs, *IEEE Transactions on Automatic Control*, vol. AC-13, no. 1, pp. 22–28, 1968.

- [32] D. Shi, T. Chen, and L. Shi, On Set-valued Kalman filtering and its application to event-based state estimation, *IEEE Transactions on Automatic Control*, vol. 60, no. 5, pp. 1275–1290, 2015.
- [33] L. Shi and A. O. Fapojuwo, TDMA scheduling with optimized energy efficiency and minimum delay in clustered wireless sensor networks, *IEEE Transactions on Mobile Computing*, vol. 9, no. 7, pp. 927–940, 2010.
- [34] L. Shi, M. Epstein, and R. M. Murray, Kalman filtering over a packet-dropping network: A probabilistic perspective, *IEEE Transactions on Automatic Control*, vol. 55, no. 3, pp. 594–604, 2010.
- [35] J. Song, D. Ding, H. Liu and X. Wang, Non-fragile distributed state estimation over sensor networks subject to DoS attacks: The almost sure stability, *International Journal of Systems Science*, vol. 51, no. 6, pp. 1119–1132, Apr. 2020.
- [36] H. Tao, H. Tan, Q. Chen, H. Liu and J. Hu,  $H_\infty$  state estimation for memristive neural networks with randomly occurring DoS attacks, *Systems Science & Control Engineering*, vol. 10, no. 1, pp. 154–165, 2022.
- [37] S. Tatikonda and S. Mitter, Control under communication constraints, *IEEE Transactions on Automatic Control*, vol. 49, no. 7, pp. 1056–1068, 2004.
- [38] L. Wang, S. Liu, Y. Zhang, D. Ding and X. Yi, Non-fragile  $l_2$ - $l_\infty$  state estimation for time-delayed artificial neural networks: An adaptive event-triggered approach, *International Journal of Systems Science*, vol. 53, no. 10, pp. 2247–2259, Jul. 2022.
- [39] L. Wang, Z. Wang, G. Wei and F. E. Alsaadi, Observer-based consensus control for discrete-time multiagent systems with coding-decoding communication protocol, *IEEE Transactions on Cybernetics*, vol. 49, no. 12, pp. 4335–4345, 2018.
- [40] G. Wei, S. Liu, Y. Song, and Y. Liu, Probability-guaranteed set-membership filtering for systems with incomplete measurements, *Automatica*, vol. 60, pp. 12–16, 2015.
- [41] P. Wen, X. Li, N. Hou and S. Mu, Distributed recursive fault estimation with binary encoding schemes over sensor networks, *Systems Science & Control Engineering*, vol. 10, no. 1, pp. 417–427, 2022.
- [42] H. S. Witsenhausen, Sets of Possible States of Linear Systems Given Perturbed Observation, *IEEE Transactions on Automatic control*, vol. 13, no. 5, pp. 556–558, 1968.
- [43] W. S. Wong and R. W. Brockett, Systems with finite communication bandwidth constraints - II: Stabilization with limited information feedback, *IEEE Transactions on Automatic Control*, vol. 44, no. 5, pp. 1049–1053, 1999.
- [44] J. Wu, L. Shi, L. Xie, and K. H. Johansson, An improved stability condition for Kalman filtering with bounded Markovian packet losses, *Automatica*, vol. 62, pp. 32–38, 2015.
- [45] L. Xie, Y. C. Soh, and C. E. De Souza, Robust Kalman filtering for uncertain discrete-time linear systems, *IEEE Transactions on Automatic Control*, vol. 39, no. 6, pp. 1310–1314, 2003.
- [46] F. Yang and Y. Li, Set-membership filtering for systems with sensor saturation, *Automatica*, vol. 45, no. 8, pp. 1896–1902, 2009.
- [47] W. Yang, C. Yang, H. Shi, L. Shi, and G. Chen, Stochastic link activation for distributed filtering under sensor power constraint, *Automatica*, vol. 75, pp. 109–118, 2017.
- [48] W. Ye, J. Heidemann and D. Estrin, Medium access control with coordinated adaptive sleeping for wireless sensor networks, *IEEE/ACM Transactions on Networking*, vol. 12, no. 3, pp. 493–506, 2004.
- [49] H. Yu, J. Hu, B. Song, H. Liu and X. Yi, Resilient energy-to-peak filtering for linear parameter-varying systems under random access protocol, *International Journal of Systems Science*, vol. 53, no. 11, pp. 2421–2436, Aug. 2022.
- [50] W. A. Zhang, L. Yu, and G. Feng, Optimal linear estimation for networked systems with communication constraints, *Automatica*, vol. 47, no. 9, pp. 1992–2000, 2011.
- [51] X.-M. Zhang, Q.-L. Han, X. Ge, D. Ding, L. Ding, D. Yue and C. Peng, Networked control systems: A survey of trends and techniques, *IEEE/CAA Journal of Automatica Sinica*, Vol. 7, No. 1, pp. 1–17, 2020.
- [52] Y. Zhao, X. He, L. Ma and H. Liu, Unbiasedness-constrained least squares state estimation for time-varying systems with missing measurements under round-robin protocol, *International Journal of Systems Science*, vol. 53, no. 9, pp. 1925–1941, Jul. 2022.
- [53] L. Zhou and G. Lu, Detection and stabilization for discrete-time descriptor systems via a limited capacity communication channel, *Automatica*, vol. 45, no. 10, pp. 2272–2277, 2009.
- [54] K. Zhu, J. Hu, Y. Liu, N. D. Alotaibi and F. E. Alsaadi, On  $l_2$ - $l_\infty$  output-feedback control scheduled by stochastic communication protocol for two-dimensional switched systems, *International Journal of Systems Science*, vol. 52, no. 14, pp. 2961–2976, 2021.
- [55] L. Zou, Z. Wang, and H. Gao, Set-membership filtering for time-varying systems with mixed time-delays under Round-Robin and Weighted Try-Once-Discard protocols, *Automatica*, vol. 74, pp. 341–348, 2016.
- [56] L. Zou, Z. Wang, H. Dong, and Q.-L. Han, Moving horizon estimation with multi-rate measurements and correlated noises, *Automatica*, vol. 30, no. 17, pp. 7429–7445, 2020.